EXPERIMENTAL INVESTIGATION OF CYCLIC RESPONSE OF STAINLESS STEEL REINFORCED CONCRETE COLUMNS

José MELO[1], Sheida AFSHAN[2], Tiziana ROSSETTO[3] & Humberto VARUM[4]

Abstract: *Corrosion of carbon steel reinforcement is the major cause of premature deterioration of reinforced concrete buildings and infrastructure. There are increasing interests in the use of maintenance-free materials such as stainless steel reinforcement in concrete, with inherent durability and resistance to various forms of corrosion and favourable mechanical properties, in particular excellent ductility and cyclic resistance. This paper presents the main results of an experimental programme designed to investigate the potential benefits of the relatively high ductility and substantial strain hardening of stainless steel on the cyclic performance of reinforced concrete columns with stainless steel reinforcing bars. Three experimental tests were performed on full-scale columns, two with duplex EN 1.4462 stainless steel reinforcement, one tested under cyclic lateral loading and one tested monotonically, and one control specimen with A500 carbon steel reinforcement tested under cyclic lateral loading. In addition, conventional pull-out tests and tensile tests were conducted for a comparative assessment of the bond and mechanical properties of the reinforcement bars. The force-displacement global response and the dissipated energy evolution of the tested columns are presented and discussed.*

Introduction

Corrosion of steel reinforcement causes premature deterioration of concrete buildings and infrastructure. This has become a major worldwide concern owing to the associated economic and environmental consequences. In the USA, the estimated annual cost of repair and maintenance in bridges alone is in excess of $8 billion (Koch et al., 2001), while in Western Europe €5 billion is spent yearly on repair works of corroding concrete infrastructure (Markeset et al., 2006). Structures located in aggressive marine environment, exposed to chloride ingress from seawater splash, e.g. sea walls, coastal defences and coastal structures (piers and docks), as well as highway bridges, roadways and parking garages, to which de-icing salts are applied during winter periods, are the most vulnerable to reinforcement corrosion. In structures with very long design life, such as historic structures and nuclear waste storage tanks, structural durability, with as low as possible maintenance requirements, is of paramount importance. In seismic areas, weakening of the reinforced concrete structures due to corrosion of reinforcement may cause early collapse of the structure in the event of an earthquake. Recent experimental studies of the cyclic behaviour of reinforced concrete elements with corroded reinforcement show that corrosion has a significant impact on the response of these structures (Kashani et al., 2017). To overcome this, stainless steel reinforcement, with inherent corrosion resistance and durability, provides a promising solution. Moreover, the high ductility and strain-hardening of stainless steel provide additional desirable characteristics for seismic applications. This paper presents an experimental investigation to study and compare the structural performance of reinforced concrete columns with stainless steel (duplex EN 1.4462 grade) and carbon steel (A500) reinforcements subjected to constant axial load and cyclic and monotonic lateral loads.

Experimental investigation

Overview

An experimental programme was carried out in the Structures Laboratory at University of Porto to investigate the structural performance of reinforced concrete columns with stainless steel

---
[1] Dr, CONSTRUCT-LESE, Faculty of Engineering, University of Porto, Porto, Portugal; EPICentre, University College London, London, UK; josemelo@fe.up.pt
[2] Dr, University of Southampton, Southampton, UK, S.Afshan@soton.ac.uk
[3] Prof., EPICentre, University College London, London, UK, t.rossetto@ucl.ac.uk
[4] Prof., CONSTRUCT-LESE, Faculty of Engineering, University of Porto, Porto, Portugal, hvarum@fe.up.pt

reinforcement bars. Three full-scale columns, two with duplex EN 1.4462 stainless steel reinforcement, and one with A500 carbon steel reinforcement subjected to constant axial compressive load and cyclic and monotonic lateral loading were tested. Material tests were performed to characterize the material properties of the reinforcement bars and the concrete used to cast the column specimens. In addition, pull-out tests on the stainless steel reinforcement bars were conducted to measure the bond strength. A description of these tests is provided hereafter.

Material tests

Three sizes of duplex EN 1.4462 stainless steel reinforcement with diameters Ø = 8 mm, 12 mm and 16 mm and two sizes of A500 carbon steel reinforcement with diameters Ø = 8 mm and 16 mm were used in the construction of the column specimens. Tensile tests were carried, in accordance with EN ISO 6892-1 (2002), to determine the basic engineering stress-strain response of these reinforcement bars. The key measured mechanical properties, including the Young's modulus E_s, the yield strength f_{sy}, taken as the 0.2% proof stress, the ultimate tensile strength f_{su} and the strain at ultimate tensile strength ε_{su} are reported in Table 1. Standard cube tests, in accordance with EN 206 (2016), were performed to measure the concrete compressive strength. Three 150 mm cube specimens were tested 90 days after casting, when the first columns test was carried out, and the average measured cube strength f_{cu} was 29.9 MPa.

Specimen reference	f_{sy} (MPa)	f_{su} (MPa)	E_s (GPa)	ε_{su} (%)
EN 1.4462-Ø8	1050	1194	181	14.0
EN 1.4462-Ø12	900	1038	192	17.0
EN 1.4462-Ø16	610	705	208	35.0
A500-Ø16	575	670	207	18.0

Table 1. Material properties of stainless steel and carbon steel reinforcements.

Pull out tests

A total of six pull-out specimens, two for each of the EN 1.4462 stainless steel reinforcement bar diameters, were cast at the same time as the column specimens. The pull-out specimens were prepared according to Annex D of EN 10080 (2005). The pull-out specimens consisted of a concrete block, with dimensions of 200 mm × 200 mm × 200 mm, and a bond length equal to five times the reinforcement bar diameter. The pull-out tests were performed using an Instron 300 DX testing machine, as shown in Figure 1. Displacements control was used to drive the testing machine at a rate of 0.17 mm/s for the 12 mm and 16 mm diameter bars and 0.10 mm/s for the 8 mm diameter bars. A LVDT was used to measure the relative displacement between the free bar end and the block concrete to obtain the slip length.

Figure 1. The pull-out test set-up.

Full-scale column tests

Three column specimens were prepared with the aim of examining the influence of reinforcement, stainless steel (SS) and carbon steel (CS), on the ultimate response of columns under combined constant axial load and cyclic (C) and monotonic (M) lateral loading conditions. Table 2 provides a summary of the conducted test programme. The columns had 300 mm × 300 mm square cross-sections with a total length of 1.65 m (column length = 1.5 m plus the length of the actuator device = 0.15 m). The columns were cast in stiff foundation blocks with dimensions of 0.44 mm × 0.44 mm × 0.50 mm, as shown in Figure 2 (a). With reference to the cantilever model, where the

inflection point is located at the column mid-height, the column and the stiff foundation block configuration adopted herein represents the behaviour of a 3.0 m height column at the base of a typical building when subjected to lateral demands induced by earthquakes (Rodrigues *et al.*, 2016). The transvers reinforcement detailing was the same in all columns as shown in Figure 2 (b). Double 8 mm stirrups closed at 135° and spaced at 0.10 m were placed at the base of the columns. The longitudinal reinforcement detailing used is explained in Table 2, which was not the same in all columns in order to have similar flexural strengths for both the stainless steel and carbon steel reinforced columns.
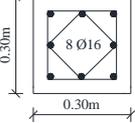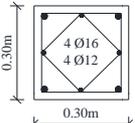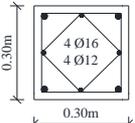
Specimen reference	Cross-section	Load type	Description
CS-C	0.30m × 0.30m, 8 Ø16	Cyclic (C)	Control specimen representative of an earthquake designed structure according to EN 1998-1:2004 (2013) for a medium seismic hazard zone and XD1/XD2/XD3 and XS1/XS2/XS3 class of exposure (corrosion induced by chlorides and corrosion induced by chlorides from sea water) with 45 mm concrete cover.
SS-C	0.30m × 0.30m, 4 Ø16 4 Ø12	Cyclic (C)	Specimen with similar flexural and shear capacities as the control specimen CS-C, but with stainless steel reinforcement and 25 mm concrete cover.
SS-M		Monotonic (M)	Same as the SS-C specimen, but subjected to monotonic lateral loading.

Table 2. Summary of the column test programme.
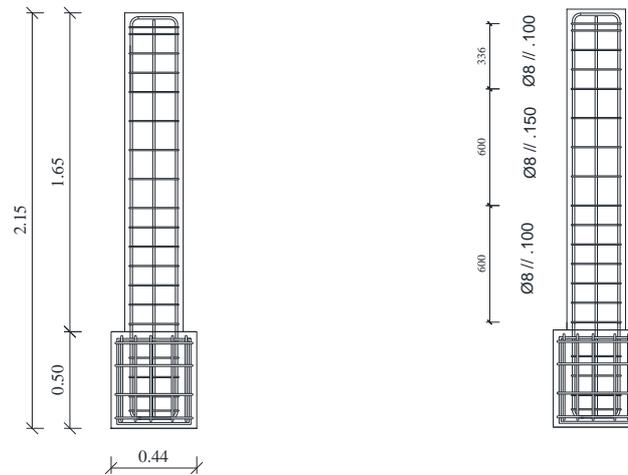
(a) Specimen dimensions.   (b) Shear reinforcement detailing.
Figure 2. Details of the specimens.

The tests we carried out in a purpose-built rig developed in the Structures Laboratory at Porto University for performing uniaxial and biaxial cyclic tests on reinforced concrete columns with constant or varying axial loads. The test rig included a vertical 700 kN capacity actuator that was used to apply the axial compressive load and a horizontal 500 kN capacity actuator with 300 mm stroke to apply the cyclic and monotonic lateral loads. The reaction system for the actuators composed of two steel reaction frames – see Figure 3. The column specimens and the reaction frames were fixed to the strong floor of the laboratory with prestressed steel bars to avoid sliding or overturning of the specimen during testing or sliding of the reaction frame. Since the axial load actuator remains in the same position during the test while the column specimen deflects laterally, a sliding device is used (placed between the top column and the actuator), which was built to minimize the friction effects. This device is composed of two sliding steel plates that exist between the top column section and the actuator. However, with the main purpose of measuring these small friction forces, a load cell in the horizontal direction was connected to the upper plate (that is expected not to displace laterally), and the corresponding measured forces (that corresponds to the friction force) were subtracted from the forces read by the load cells of the horizontal actuator. The local displacements at the column plastic hinge region were measured by several

potentiometers – see Figure 3. Four strain gauges were placed on the corner longitudinal reinforcing bars at 5 cm from the top block foundation. The rotation of the column foundation block was measured during the test using an inclinometer sensor, which were in turn used to correct the imposed lateral displacements at the top of the column and compute the real imposed drift.
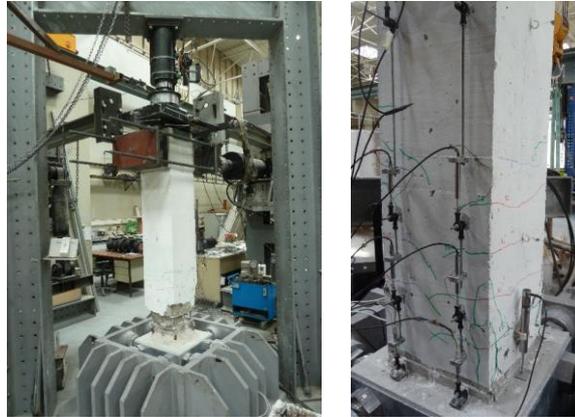

Figure 3. Column test set-up and load monitoring.

Lateral displacements were imposed at the top of the columns. Three cycles were repeated for each lateral deformation demand level, with steadily increasing demand levels. This procedure was adopted to obtain a better understanding of the behaviour of the columns and allowed comparisons between different tests to be made. Furthermore, it provided the relevant information for the development and calibration of numerical models for future numerical modelling investigations. The adopted lateral load path followed the nominal peak displacement levels of: 3, 5, 10, 4, 12, 15, 7, 20, 25, 30, 35, 40, 45, 50, 55, 60, 65, 70, 75 (in mm). The axial load was set to a constant value of 515 kN which corresponds to an axial load ratio of 19%.

Experimental results and discussions

Lateral force-imposed drift relationship

The lateral force-drift relationships obtained from the column tests are presented in Figure 4. Figure 4 (a) compares the responses of the columns with stainless steel reinforcement subjected to monotonic and cyclic lateral loadings i.e. specimens SS-C and SS-M, while Figure 4 (b) compare the responses of the columns with stainless steel and carbon steel reinforcement, specimens CS-C and CS-S, respectively, subjected to cyclic lateral loading. The flexural capacities of the tested columns corresponding to the applied maximum lateral loads, determined according to the EN 1992-1-1 (2010) formulations, assuming plane cross-section and perfect bond conditions, are also included Figure 4, as depicted by the red and black horizontal lines.

Table 3 summarizes the key response values (for positive direction) for the tested columns, including the maximum force $F_{c,max}$, the drift at maximum force $Drift_{Fc,max}$, the ultimate force $F_{c,ult}$ and the drift at ultimate force $Drift_{ult}$. The ultimate point was conventionally taken as the point at which a strength reduction of 20%, relative to the maximum force applied, was observed as adopted by Park and Ang (1987). For the SS-M specimen, subjected to monotonic loading, the maximum strength reduction at the end of the test was 11% (corresponding to 6.0% drift), and consequently the conventionally defined ultimate point was not reached.

The envelope of the cyclic response for the SS-C specimen and the monotonic response for the SS-M specimen are similar until 2.3% drift, where the SS-C column reaches the maximum lateral force – see Figure 4(a). For larger drifts beyond this point, there is softening until 4.3% drift (i.e. at the ultimate point) for the SS-C column, while the SS-M column exhibits a plateau until 4.2% drift, followed by a small reduction in strength until 6.0% drift (i.e. at the end of test). Therefore, while the cyclic loading applied does not affect the maximum strength of the SS-M and SS-C specimens significantly, it reduces the ductility of the SS-C specimen. The EN 1992-1-1 maximum strength prediction is 95.0 kN which is slightly lower than the measured values, 95.9 kN and 99.0 kN for SS-C and SS-M columns, respectively.

As shown in Figure 4(b), the CS-C column reached its maximum force $F_{c,max}$ and ultimate force $F_{c,ult}$ at significantly lower drift demands than the SS-C column ($Drift_{Fc,max}$ = 1.7% and $Drift_{ult}$ =

3.3% for CS-C against $Drift_{Fc,max}$ = 2.3% and $Drift_{ult}$ = 4.2% for SS-C). This is due to the lower yield stress of the carbon steel reinforcement and the larger concrete cover of the CS-C specimen and the higher strain at ultimate tensile stress of the 16 mm diameter stainless steel reinforcement of the SS-C specimen. The initial stiffness and the pinching effect are similar in both the CS-C and the SS-C columns. The global cyclic performance of the SS-C column is better than that of the CS-C columns since it sustained larger ultimate drift (i.e. higher ductility) and exhibits less softening. The measured maximum strength of the CS-C column was 91.2 kN, which is comparable to the EN 1992-1-1 predicted value of 88.3 kN. Therefore, the EN 1992-1-1 design predictions were shown to be accurate for both carbon steel and stainless steel specimens.
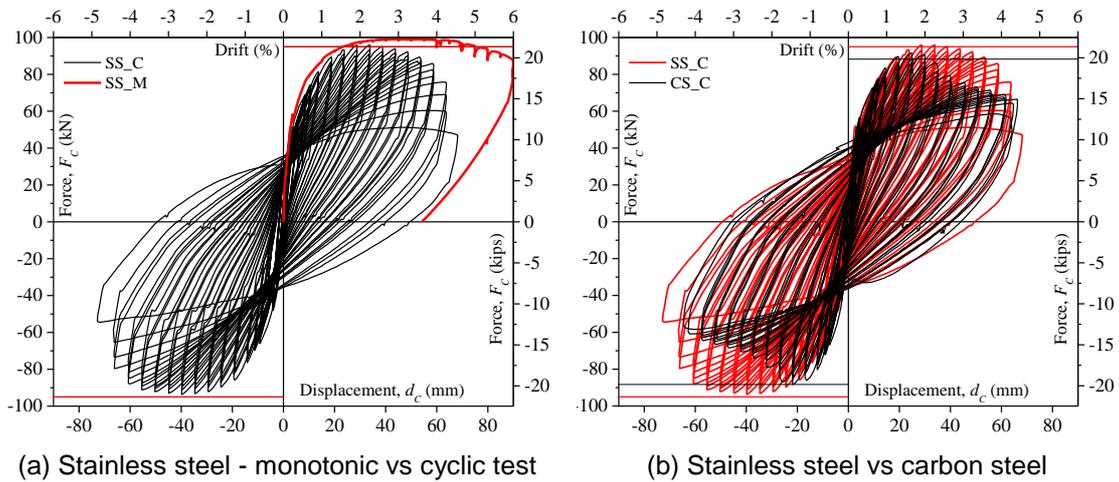

(a) Stainless steel - monotonic vs cyclic test   (b) Stainless steel vs carbon steel

Figure 4. Comparison of the measured lateral force-drift relationships.

Specimen	$F_{c,max}$ (kN)	$Drift_{Fc,max}$ (%)	$F_{c,ult}$ (kN)	$Drift_{ult}$ (%)
CS-C	91.2	1.7	73.0	3.3
SS-C	95.9	2.3	76.8	4.2
SS-M	99.0	2.9	-	-

Table 3. Measured force and drift value for the maximum strength and ultimate points.

Hysteretic dissipated energy evolution

Figure 5 shows the evolution of the hysteretic energy dissipated for the CS-C and SS-C columns, computed from the experimental results, with the energy dissipated at the ultimate drift values also distinctly marked. The hysteretic dissipated energy evolution is similar for both specimen until 2.5% drift, beyond which, the CS-C column tends to dissipate more energy due to the larger damage observed during the test. However, the SS-C specimen (with stainless reinforcement bars) dissipated 56% more energy than the CS-C specimen at the ultimate point, hence evidencing the superior cyclic performance of SS-C. This large difference is essentially due to the larger ultimate drift of the SS-C column. At the end of the tests, the total hysteretic dissipated energy and the drift demands were similar for both CS-C and CS-S columns.
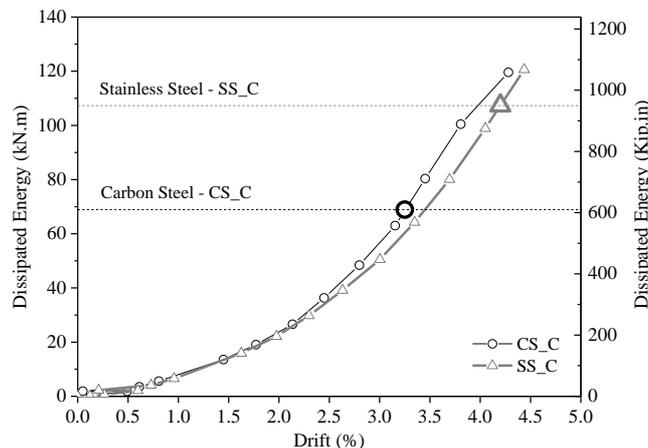

Figure 5. Dissipated energy evolution of the cyclic tests.

Damage observed

Table 4 illustrates the damage patterns observed for each of the specimens at the end of the test. In all specimens, concrete spalling was observed in the plastic hinge zone along 36 cm, 40 cm and 27 cm for the CS-C, SS-C and SS-M columns, respectively. Evident buckling of the reinforcement bars was observed in the specimens subjected to cyclic lateral loading (CS-C and SS-C). The distribution of the cracks was similar on the CS-C and SS-C columns, which indicates that the slippage was identical in both specimens. When slippage occurs, plastic hinge length tends to be smaller and the cracks are more concentrated at the base of the column. This indicates similar bond-slip relationship for ribbed stainless steel and carbon steel. For the SS-M column, flexural and some shear cracks were observed in the concrete zone under tensile stress.

| | Carbon Steel | Stainless Steel | |
	CS-C (Cyclic)	SS-C (Cyclic)	SS-M (Monotonic)
Global view			
Lateral view			
Front view			

Table 1. Damage observed at the end of the column tests.

Pull-out tests and adapted bond-slip proposal

Figure 6 presents the results of the pull-out tests performed on the 6 stainless steel specimens. The aim of these tests was to assess the bond-slip relationship of the stainless steel reinforcement bars and to compare with the theoretical bon-slip model for carbon steel hot rolled ribbed reinforcement bars proposed by Eligehausen et al. (1983) for unconfined concrete. The model is for good bond conditions and includes a non-linear initial branch as given by Equation (1) until s_{max}, defined as the slip value corresponding to the maximum bond stress $\tau_{b,max}$, followed by a second constant branch. The maximum bond stress ($\tau_{b,max}$) depends on the characteristic cylindrical concrete compressive strength f_{ck} (in MPa). In this study, f_{ck} = 22 MPa was assumed

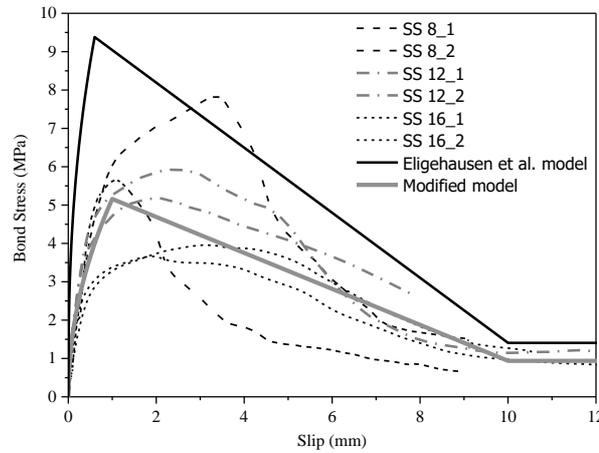(i.e. the mean measured value of the concrete cube strength 29.9 MPa minus 8 MPa, according to EN 1992-1-1).

Figure 6. Pull-out test results: bond stress-slippage relationship.

From Figure 6 it is observed that the maximum bond stress $\tau_{b,max}$ obtained for the tested stainless steel reinforcement bars is lower than the predicted stress based on the Eligehausen et al. (1983) model proposed for carbon steel reinforcement bars. Moreover, the slip at maximum bond stress s_{max} is also larger for the tested stainless steel reinforcement bars. More pull-out tests should be carried out to allow a robust bond-slip relationship for stainless reinforcement bars to be proposed. However, based on the results obtained herein, the Eligehausen et al. (1983) model depicted in Figure 7 was modified for stainless reinforcement bars and the proposed modified model is presented in Figure 6. The original bond-slip model parameters and the proposed modified model parameters for stainless steel reinforcement bars are presented in Table 5. The proposed parameters are valid for unconfined concrete and good bond conditions.
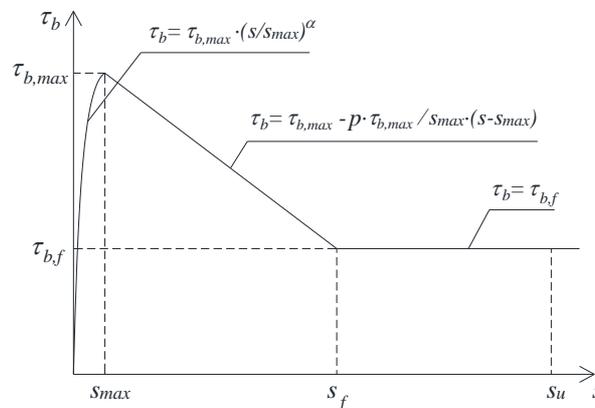

Figure 7. Bond-slip relationship for hot rolled carbon reinforcing bars Eligehausen et al. (1983).

$$\tau_b = \tau_{b,\max} \cdot \left(\frac{s}{s_{\max}} \right)^\alpha \tag{1}$$

where τ_b is the bond stress, $\tau_{b,max}$ is the maximum bond stress, s is the slippage, s_{max} is the slippage at maximum bond stress and α is the empirical factor defining the shape of the branch.

Model	$\tau_{b,max}$ (Mpa)	s_{max} (mm)	$\tau_{b,f}$ (Mpa)	s_f (mm)	α
Eligehausen et al. (1983) model	$2.0\sqrt[2]{f_{ck}}$	0.60	$0.3\sqrt[2]{f_{ck}}$	10	0.40
Adapted model for stainless steel	$1.1\sqrt[2]{f_{ck}}$	1.00	$0.2\sqrt[2]{f_{ck}}$	10	0.50

Table 2. Bond-slip model parameters.

Conclusions

The work presented in this paper assessed the performance of reinforced concrete columns with carbon steel (A500) and stainless steel reinforcement (EN 1.4462) bars subjected to constant compressive axial load and monotonic and cyclic lateral loading conditions. Moreover, tensile tests were performed on the reinforcement bars to measure the key material characteristics. Six pull-out tests were carried out on samples with stainless reinforcement bars to measure the bond-slip behaviour. The main conclusions are summarized as follow:

- The maximum strengths of the columns with carbon steel and stainless steel reinforcement bars subjected to constant compressive axial and cyclic lateral loads were similar and comparable to those predicted from the EN 1992-1-1 guidelines.

- The global behaviors of the SS-C and SC-C columns were similar until the maximum strength point, beyond which the softening was more evident for the CS-C column and therefore the ultimate drift was 22% lower than for the SS-C column.

- The stainless steel reinforced concrete column tested monotonically (SS-M) presented similar force-drift relationship to that tested cyclically (SS-C) until the maximum force was reached following which, the SS-M column showed a large plateau response, indicating the higher ductility of the SS-M column compared to the SS-C column.

- The SS-C column dissipated 56% more energy than the CS-C column until the ultimate strength point. This shows that the use of stainless steel may not affect the cyclic performance and might be used on regions with medium to high seismic hazard.

- The damage observed on both columns tested cyclically were comparable as well as the extension of concrete spalling. Buckling of the longitudinal bars was also observed in both columns.

- The results of the pull-out tests have shown lower maximum bond stress and larger slippage at maximum bond stress than the predictions given by the bond-slip model developed by Eligehausen et al. (1983) for carbon reinforcing steel bars.

- An modified bond-slip model is proposed for stainless reinforcing bars.

This work has demonstrated the superior ductility and energy dissipation capacity of columns with stainless steel reinforcement, which coupled with the excellent corrosion resistance properties of the material, brings about clear benefits for future use of stainless steel reinforcement in RC structures in aggressive environments and subjected to seismic loading.

Acknowledgements

References

EN ISO 6892-1 (2016) *Metallic materials – tensile testing. Part 1: Method of test at room temperature*. European Committee for Standardization. Brussels.

EN 206:2013+A1 (2016) *Concrete – Specification, performance, production and conformity*. European Committee for Standardization. Brussels.

EN 10080 (2005) *Steel for the reinforcement of concrete – Weldable reinforcing steel – General*. European Committee for Standardization. Brussels.

EN 1998-1:2004+A1 (2013) *Eurocode 8: Design of structures for earthquake resistance – Part 1: General rules, seismic actions and rules for buildings*. European Committee for Standardization. Brussels.

EN 1992-1-1 (2010) *Eurocode 2: design of concrete structures. Part 1-1: General rules and rules for buildings*. European Committee for Standardization. Brussels.

Park YJ, Ang AHS and Wen YK (1987) Damage-limiting aseismic design of buildings. *Earthquake Spectra,* 3(1):1-26.

Eligehausen R, Popov EP and Bertero VV (1983) *Local bond stress–slip relationships of deformed bars under generalized excitations.* EERC University of California, Berkeley, Report No. UCB/EERC 83-23.

Kashani MM, Crewe AJ and Alexander NA (2017) Structural capacity assessment of corroded RC bridge piers, *Proceedings of the Institution of Civil Engineers – Bridge Engineering*, 170(1): 28-41.

Koch GH, Brongers MPH, Thompson NG, Virmani YP and Payer JH (2001) Corrosion costs and preventive strategies in the United States, Publication No. FHWA-RD-01-156.

Markeset G, Rostam S and Klinghoffer O (2006) Guide for the use of stainless steel reinforcement in concrete structures, Nordic Innovation Centre project-04118.

Rodrigues H, Furtado A and Arête A (2016) Behavior of Rectangular Reinforced-Concrete Columns under Biaxial Cyclic Loading and Variable Axial Loads, *Journal of Structural Engineering*, 142(1): 04015085.